Cell. Mol. Life Sci. 64 (2007) 498 – 505
1420-682X/07/040498-8
DOI 10.1007/s00018-007-6449-8

Cellular and Molecular Life Sciences

Research Article

Alcohol dehydrogenase 2 is a major hepatic enzyme for human retinol metabolism

M. Hellgren[a], P. Strömberg[a, +], O. Gallego[b, ++], S. Martras[b], J. Farrés[b], B. Persson[c, d], X. Parés[b] and J.-O. Höög[a, *]

[a] Department of Medical Biochemistry and Biophysics, Karolinska Institutet, 171 77 Stockholm (Sweden), Fax: +468-337 462, e-mail: jan-olov.hoog@ki.se
[b] Department of Biochemistry and Molecular Biology, Universitat Autònoma de Barcelona, 08193 Bellaterra, Barcelona (Spain)
[c] IFM Bioinformatics, Linköping University, SE-581 83 Linköping (Sweden)
[d] Department of Cell and Molecular Biology, Karolinska Institutet, 171 77 Stockholm (Sweden)

Received 12 October 2006; received after revision 6 December 2006; accepted 8 January 2007
Online First 5 February 2007

Abstract. The metabolism of all-*trans*- and 9-*cis*-retinol/retinaldehyde has been investigated with focus on the activities of human, mouse and rat alcohol dehydrogenase 2 (ADH2), an intriguing enzyme with apparently different functions in human and rodents. Kinetic constants were determined with an HPLC method and a structural approach was implemented by *in silico* substrate dockings. For human ADH2, the determined K_m values ranged from 0.05 to 0.3 μM and k_{cat} values from 2.3 to 17.6 min^{-1}, while the catalytic efficiency for 9-*cis*-retinol showed the highest value for any substrate. In contrast, poor activities were detected for the rodent enzymes. A mouse ADH2 mutant (ADH2Pro47His) was studied that resembles the human ADH2 setup. This mutation increased the retinoid activity up to 100-fold. The K_m values of human ADH2 are the lowest among all known human retinol dehydrogenases, which clearly support a role in hepatic retinol oxidation at physiological concentrations.

Keywords. Alcohol dehydrogenase, computer modeling, kinetic constant, retinaldehyde, retinol, substrate docking.

Introduction

Retinoids are essential in cell development and growth as well as for maintenance of adult epithelia and in vision. The proposed active forms in cell signaling are the oxidized forms, all-*trans*- and 9-*cis*-retinoic acids, which bind to their nuclear receptors [1, 2], although the role of 9-*cis*-retinoic acid in retinoid signaling recently has been questioned [3]. The conversion into the corresponding active forms is performed in two steps in which retinol is first oxidized to retinaldehyde, and then further oxidized to retinoic acid. The enzymes involved in the first step of retinol conversion, the rate-limiting step, belong to the alcohol dehydrogenase (ADH) and/or short-chain dehydrogenase/reductase (SDR) families [4–6]. Recently, aldo-keto reductases (AKR) have been added to the group of retinoid metabolizing enzymes, but they seem primarily to be involved in retinaldehyde reduction [7, 8].

[+] Present address: AstraZeneca R&D, 151 85 Södertälje (Sweden)
[++] Present address: EMBL, Meyerhofstrasse 1, 69117 Heidelberg (Germany)
* Corresponding author.

Retinol dehydrogenases (RDH) from the SDR family are mainly microsomal enzymes that are dependent on either NAD(H) or NADP(H) for activity. It has been suggested that the RDHs within this group oxidize retinol bound to cellular retinol-binding protein (CRBP), which harbors the major part of retinol in the cell, and with this in view several reports have argued for a role of SDR-RDHs in this conversion [2, 9]. In addition, genetic studies have shown that CRBP actively participates in retinyl ester storage and that ADH antagonizes this process by metabolizing free retinol [2, 4, 10]. Recently, in a comparison between different retinoid-metabolizing enzymes performed under identical conditions with a newly developed method, doubts have been raised as to whether the complex CRBP-retinol would even be a favorable substrate for retinol oxidation at all [8]. The second step in retinoic acid formation is catalyzed by cytosolic retinaldehyde dehydrogenases that irreversibly oxidize retinaldehyde to the acid form [11].

Within the mammalian ADH family, a system divided into classes (ADH1–5), isoenzymes and allelic forms, mainly ADH1 and ADH4 have been ascribed active functions in retinol oxidation. ADH4, the non-hepatic form of mammalian ADH, has a very high turnover rate for retinols [5, 8, 12, 13]. The human ADH enzymes have been investigated for retinol metabolism [4, 5, 14] and all except ADH3, defined also as glutathione-dependent formaldehyde dehydrogenase and nitroso-glutathione reductase [5, 6], show a clear capacity for retinoid conversion. However, it was recently shown that also ADH3 is able to catalyze retinol oxidation, albeit with a very low activity, and knockout mice studies suggest that ADH3 actively participates in this metabolism [15]. ADH2 has been an enigma because of its different characteristics in human and rodents. The human form is active against several metabolites, *e.g.*, in retinoid oxidoreduction and 4-hydroxynonenal reduction, whereas the rodent enzymes almost lack alcohol oxidation and aldehyde reduction capacity [6, 16]. This is related to the unique fact that rodent ADH2 enzymes show a proline residue at position 47, rather than histidine (human) or arginine (rabbit) [16, 17]. Because mice have been used as the main model system for retinoid studies [4, 12], and it was suggested that mouse lacked ADH2, the isolation and kinetic characterization of this ADH as well as its structural determination [16, 18] are of great importance to understand retinoid metabolism in rodents.

The contribution of ADH2 in cell signaling, *i.e.*, retinol oxidation, has been studied here with all-*trans*- and 9-*cis*-retinol/retinaldehyde as substrates for human, mouse and rat ADH2 as well as for a mouse ADH2Pro47His mutant. The kinetic studies were performed with a newly developed method based on high-sensitivity HPLC analyses of formed product and addition of bovine serum albumin (BSA) to solubilize retinoids [8, 19]. In addition, alcohol substrates tested were docked *in silico* to models of the ADH2 enzymes to explain binding properties. The results suggest that human ADH2 is a major hepatic retinol dehydrogenase, whereas the rodent ADH2s are of minor importance in retinoid metabolism.

Materials and methods

Expression and isolation of human and rodent ADH2. Recombinant proteins were expressed in 2-l LB cultures of *Escherichia coli* strain BL21(DE3) at 37°C overnight, according to Svensson et al. [16]. Isolation of proteins from the cell lysates were carried out in three steps: DEAE-cellulose (DE-52, 2.6 cm×20 cm column; Whatman, UK) in 0.1 M Tris-HCl, pH 8.0; AMP-Sepharose (1.6 cm×6 cm column; Amersham Biosciences, Sweden), where the bound proteins were eluted with 5.0 mM NAD^+, 0.2 M NaCl in 10 mM Tris-HCl, pH 8.0; and HiLoad Superdex 200 (16/60 prep grade; Amersham Biosciences), in 0.2 M NaCl, 1 mM DTT and 10 mM Tris-HCl, pH 8.0. All protein preparations were homogeneous as determined by SDS-polyacrylamide gel electrophoresis.

Activity measurements. Retinol and retinaldehyde assays were performed at 37°C in 0.5–2-ml reaction volumes, in 0.1 M phosphate buffer, pH 7.5, and 2.3 mM NAD^+ or NADH, coenzyme concentration that will saturate the ADH2 enzymes [20]. Retinoids were prepared and concentration determined as described [8, 12, 19]. The retinoid concentration was in an interval of 0.1–10 times the K_m (0.01–10 μM) with BSA in a 1:1 ratio to retinoid concentration as a stabilizer [19]. Activity measurements were stopped with two reaction volumes of cold methanol after 15 min or up to 60 min for reactions with low turnover rates. For extraction of retinoids, one volume of hexane was added and the reaction mixture was vortexed and briefly centrifuged. The retinoids were separated by normal-phase HPLC Spherisorb S3W column (4.6 mm×100 mm) with a mobile phase of hexane/*tert*-butyl-methyl ether (96:4) at a flow rate of 2 ml/min [8, 19]. Analysis was performed with a Waters 2996 Photodiode Array Detector. Retinoids were quantified by comparing their peak areas to a calibration curve constructed from peak areas of a series of a standard [19]. The activities were measured in a double sample set of at least five different concentrations and only values below 10% of conversion (below 20% for the lowest substrate concentrations) were accepted to approximate to initial velocity measurements. No deviation from linearity was observed under these conditions [19, 21]. For reactions with low turnover rates, especially those with rodent enzymes, a higher protein concentration and prolonged reaction time were used to determine reaction velocities, even though it was not possible to determine K_m and k_{cat} values for the reactions with the lowest activities. The spectrophotometric assay, at 400 nm, was used for kinetic determinations with Tween 80 (0.02%, v/v) as a solubilizer and stabilizer instead of BSA, under the same conditions as for the HPLC assays. The experiments with Tween 80 were performed to relate results to earlier published values [14, 19]. Retinoid concentration was measured using the specific molar absorption coefficients [8, 14, 19, 22, 23]. Protein concentrations were determined with the Bio-Rad protein assay, standardized with BSA, complemented with amino acid analysis on an Amersham Pharmacia Biotech Alpha Plus Analyzer. The kinetic constants were calculated with the software SigmaPlot (version 8.0, Enzyme plug-in, Systat Software GmbH, Germany) using a nonlinear regression fit to the standard Michaelis-Menten equation and a standard error of less than 20% was accepted.

Alignment, homology modeling and docking. Alignment of mouse, rat and human ADH2 sequences was produced with the program ICM (version 2.7, Molsoft LLC, San Diego) using the ZEGA

algorithm, with the Gonnet matrix and gap/extension penalties of 2.4/0.15. Only one 1-residue gap (residue Ala61 in human ADH2) and one 2-residue gap (residues Lys304-Gly305 in human ADH2) were obtained between the mouse and human sequences, and no gap between the mouse and rat sequences. The residue identities were 73% between mouse and human ADH2, and 93% between mouse and rat ADH2.

The program ICM was further used for molecular modeling and substrate docking. Homology models were calculated for human and rat ADH2, using mouse ADH2 as a template (PDB entry 1e3e; [18]), according to earlier ADH modeling experiments [24]. For mouse ADH2, hydrogen atoms were added and followed by a short energy minimization to avoid clashes between the added hydrogen atoms and other atoms in the structure. Evaluation of the homology models and the template structure was performed with the programs WhatIf and Procheck [25, 26], and no significant difference in structural quality between the template and the homology models were obtained. The total calculated electrostatic energies and van der Waals energies for the homology models were of the same range as that for the template structure, showing that unacceptable atom clashes in the models were avoided.

All-*trans*- and 9-*cis*-retinol were docked into mouse, rat and human ADH2. In addition, the structurally determined *N*-cyclohexylformamide (CXF) mouse ADH2 complex [18] was used as a control to test the reliability of the method. The overall distances between CXF and atoms in the vicinity of the active-site zinc correlated well between docking experiments and the X-ray determined structure. Non-rigid docking calculations were performed allowing free movement of the substrate, free rotation of selected bonds within the substrate and free rotation of the side chains along the substrate pocket [24]. Three distance restraints were imposed to guide the substrate into the active site pocket: between the oxygen of the substrate OH group and the active site zinc, between the hydrogen of the substrate OH and the oxygen of the Thr48 side chain, and between the donor hydrogen of the substrate and the acceptor carbon of the cofactor NAD^+. To further validate the docking, four different start positions for the substrate in relation to the protein were chosen and the standard deviations for the final distances between certain atoms were calculated.

Results

The conversion of retinoids differs widely between ADH2 enzymes from various mammalian species, and the human ADH2 exhibited the highest activity for each of the substrates tested, all-*trans*-retinol/retinaldehyde and 9-*cis*-retinol/retinaldehyde (Table 1). The results from this study showed the lowest K_m values obtained so far for an ADH in the metabolism of retinoids. The accurate determination of these values requires a highly sensitive method, such as the HPLC technique [8, 19] used here.

For the human enzyme, the overall range for k_{cat}/K_m was 7.9–330 μM^{-1} min^{-1} with 9-*cis*-retinol, which represented by far the best retinoid substrate (Table 1). In fact, the k_{cat}/K_m value for 9-*cis*-retinol was the highest for any alcohol or aldehyde substrate tested so far, including benzoquinones [16]. In general, all retinoid alcohols were better substrates as compared to the corresponding aldehydes (Tables 1 and 2), with both lower K_m and higher k_{cat} values. Mouse ADH2 could not be saturated with any of the retinoids tested and exhibited rates ranging from 500 to 9000-fold lower than the human enzyme (Table 2). The rat enzyme showed low activity towards all-*trans*-retinoids but for 9-*cis*-retinol/retinaldehyde it was possible to calculate K_m and k_{cat} values (Table 1). The mutated mouse ADH2 form, which has a Pro47His substitution that makes the enzyme more similar to the human form (Fig. 1), showed 5–150-fold increased activities compared to the native enzyme, although these were still lower than the values for human ADH2 (Table 2). All the determined K_m values were in the low micromolar range, 0.054–0.65 μM (Table 1). Comparison of the activity of mouse ADH2 (25–38 pmol/min/mg protein) for retinols places this enzyme in the same group as ADH3 as compared to the high activity forms, ADH1 and ADH4, where human ADH2 is found (Table 2). With Tween 80 instead of BSA as a stabilizer for the retinoids tested, the K_m values obtained were increased up to 100-fold (Table 1), while no change was detected in the k_{cat} values.

Docking experiments of substrates were performed in the dimer models of the different ADH2s (Fig. 2). Some crucial atomic distances for the catalysis of substrates in ADH are presented in Table 3. These are the distances between the hydroxyl oxygen (O) of the substrate and the active site zinc (ZN), and the distance between the cofactor NAD^+ carbon atom (C4N), at the *para* position in the nicotinamide ring and one of the hydrogen atoms (H_{15A}/H_{15B}) of the last carbon in the alcohol chain. The distances that were determined in the docking experiments for all-*trans*- and 9-*cis*-retinol are almost identical in the three different species variants of ADH2 (Table 3, Fig. 3). The docking of substrates to ADH2Pro47His mutant (not included in Table 3) did not reveal any difference with the native mouse dockings. All binding/interaction distances in the inner part of the substrate-binding pocket were in the range 2.1–2.6 Å.

The relatively high standard deviations of the distances, between the C15 of the substrate and the zinc (ZN) atom and also between the hydroxyl oxygen (O) of the substrate and the hydroxyl hydrogen (H) of Thr48, indicate a possible two-conformation state for 9-*cis*-retinol in the active site pocket (Table 3, Fig. 3b). For all-*trans*-retinol, this two-conformation state can also be observed as a minor rotation of all-*trans*-retinol in the active site (Fig. 3a).

Of the six amino acid residues in the substrate-binding pocket, which were shown to be in contact with the substrate analogue CXF [18], two differ between the human ADH2 and the rodent forms. Position 93 harbors Tyr in the human ADH2 and Phe in rodent forms, which changes the environment, and the docking experiments showed a clear interaction for rat ADH2 with all-*trans*- and 9-*cis*-retinol at this

Table 1. Kinetic constants of ADH2 enzymes with retinoids[a]

Substrate	Constant	Units	Human ADH2	Rat ADH2	Mouse ADH2	ADH2P47H
All-*trans*-retinol	K_m	μM	0.14 ± 0.02 (12)	LA	LA	0.13 ± 0.04
	k_{cat}	min^{-1}	4.0 ± 0.2	LA	LA	0.50 ± 0.14
	k_{cat}/K_m	$\mu M^{-1} \cdot min^{-1}$	29			3.8
All-*trans*-retinaldehyde	K_m	μM	0.29 ± 0.03 (11)	LA	LA	LA
	k_{cat}	min^{-1}	2.3 ± 0.1	LA	LA	LA
	k_{cat}/K_m	$\mu M^{-1} \cdot min^{-1}$	7.9			
9-*cis*-retinol	K_m	μM	0.054 ± 0.001 (5)	0.57 ± 0.08	LA	LA
	k_{cat}	min^{-1}	17.6 ± 0.6	0.98 ± 0.04	LA	LA
	k_{cat}/K_m	$\mu M^{-1} \cdot min^{-1}$	330	1.7		
9-*cis*-retinaldehyde	K_m	μM	0.21 ± 0.06 (11)	0.65 ± 0.1	LA	LA
	k_{cat}	min^{-1}	3.2 ± 0.2	0.58 ± 0.1	LA	LA
	k_{cat}/K_m	$\mu M^{-1} \cdot min^{-1}$	15	0.89		

[a] All values were determined in 0.1 M sodium phosphate buffer, pH 7.5, and 2.3 mM NAD^+/NADH at 37°C with BSA in a 1:1 ratio to retinoids. The k_{cat} values were determined per dimer (80 kDa). The K_m and k_{cat} values are given as the mean ± SE (standard error) and calculated with SigmaPlot. K_m values for human ADH2 within parenthesis were determined spectrophotometrically with Tween 80 as a solubilizer and stabilizer. Reaction rates with too low activity to determine K_m and k_{cat} values are denoted low activity (LA).

Table 2. Reaction rates for the different ADH2 enzymes in comparison to mouse ADHs[a]

Substrate	Human ADH2	Rat ADH2	Mouse ADH2	ADH2P47H
All-*trans*-retinol (5.2 μM)	48 600	6100	38	5800
All-*trans*-retinaldehyde (6.2 μM)	27 500	500	50	250
9-*cis*-retinol (7.6 μM)	220 000	11 400	25	3800
9-*cis*-retinaldehyde (4.8 μM)	38 000	6400	40	380
	Mouse ADH1	ADH3	ADH4	
All-*trans*-retinol (30 μM)	150 500	105	422 000	

[a] Reaction rates presented as amount of converted substrate in pmol/min/mg protein at a single substrate concentration. All values were determined in 0.1 M sodium phosphate buffer, pH 7.5, and 2.3 mM NAD^+/NADH at 37°C with BSA in a 1:1 ratio to retinoid. The retinoid substrate concentrations were >20-fold higher than the determined human ADH2 K_m values. The same substrate concentration for each retinoid was used to compare reaction rates between species. The reaction rate for mouse ADH1, ADH3 and ADH4 with all-*trans*-retinol are shown for comparison [15]

position. The other residue that differs is Phe/Met at position 141. This exchange will make the substrate-binding pocket much narrower in the rodents and the residue at this position showed contacts in the docking experiments in all tested structures. All residues postulated to line the entrance of the substrate-binding pocket differed between the rodent forms and the human ADH2 (Fig. 1), in which several are in close contact with the docked substrates. From the other subunit, a few residues (309-311 in human ADH2, and 308, 309 and 312 in the rodent forms, also with differences) showed weak van der Waals interactions with both all-*trans*- and 9-*cis*-retinol.

Discussion

All-*trans*-retinoic acid is a powerful hormone synthesized in a variety of tissues [1, 2, 11]. Oxidation of retinol to retinaldehyde determines the overall rate of retinoic acid formation, a reaction that is catalyzed by multiple dehydrogenases/reductases. In this study we focused on the capability of mammalian ADH2 as a retinol dehydrogenase. The K_m and k_{cat} values for retinoids with human ADH2 were determined to be in the range of 0.05–0.3 μM and 2.3–17.6 min^{-1}, respectively. The k_{cat} values of human ADH2 for retinol oxidation are comparable to those for aliphatic alcohols at pH 7.5 [16], thus suggesting a common rate-limiting step, probably the dissociation of cofac-

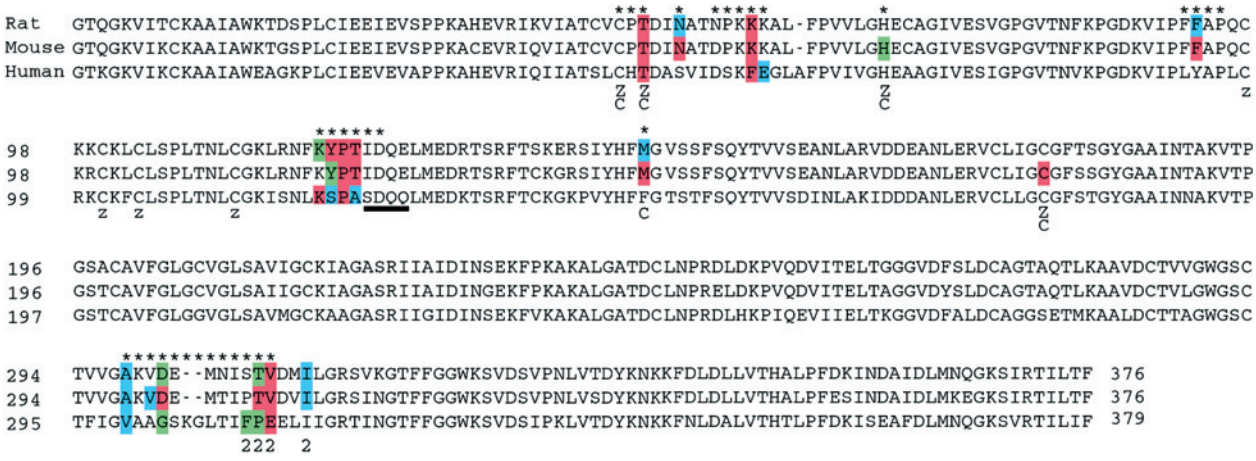

Figure 1. Alignment of human and rodent ADH2 with ICM. Stars (*) give all residues with free rotation of their side chain in the docking experiments. Residues with a distance <3.0 Å to the active site zinc (PDB entry 1e3e) are labeled with (Z) and to the structural zinc with (z). Residues with a distance <3.0 Å to CXF (PDB entry 1e3i) are labeled with (C). Coloring of residues: red are within 3.0 Å to both all-*trans*- and 9-*cis*-retinol, green are within 3.0 Å only to all-*trans*-retinol, and blue are within 3.0 Å to 9-*cis* retinol. Gaps are indicated with (-) and residues labeled with (2) are from the other monomer in the dimer and within 3.0 Å to the substrate. The four-residue insertion typical for mammalian ADH2 is underlined, showing its close vicinity to retinoid binding residues.

Table 3. Docking of retinoids in ADH2[a]

Substrate		Protein/Cofactor/Zn		Human ADH2		Rat ADH2		Mouse ADH2	
Group	Atom	Group	Atom	Distance ± SD (Å)		Distance ± SD (Å)		Distance ± SD (Å)	
AT-RetOH	C_{15}	Thr48	C_B	4.7	± 0.2	4.7	± 0.1	4.5	± 0.1
9C-RetOH	C_{15}	Thr48	C_B	4.7	± 0.2	4.9	± 0.2	4.8	± 0.2
AT-RetOH	C_{15}	NAD^+	C4N	3.5	± 0.1	3.5	± 0.1	3.5	± 0.1
9C-RetOH	C_{15}	NAD^+	C4N	3.3	± 0.2	3.5	± 0.2	3.3	± 0.1
AT-RetOH	C_{15}	Zn	ZN	3.6	± 0.1	3.4	± 0.1	3.5	± 0.1
9C-RetOH	C_{15}	Zn	ZN	3.5	± 0.4	3.5	± 0.6	3.5	± 0.4
AT-RetOH	H_{15A}	NAD^+	C4N	**2.5**	**± 0.1**	**2.4**	**± 0.0**	**2.4**	**± 0.0**
9C-RetOH	H_{15A}	NAD^+	C4N	**2.5**	**± 0.1**	**2.6**	**± 0.1**	**2.5**	**± 0.1**
AT-RetOH	H_{15B}	NAD^+	C4N	3.8	± 0.1	4.0	± 0.1	4.2	± 0.1
9C-RetOH	H_{15B}	NAD^+	C4N	4.2	± 0.1	4.2	± 0.2	4.2	± 0.1
AT-RetOH	O	Zn	ZN	**2.3**	**± 0.0**	**2.1**	**± 0.0**	**2.2**	**± 0.1**
9C-RetOH	O	Zn	ZN	**2.5**	**± 0.1**	**2.5**	**± 0.1**	**2.5**	**± 0.1**
AT-RetOH	O	Thr48	H	3.9	± 0.2	3.4	± 0.2	2.8	± 0.1
9C-RetOH	O	Thr48	H	3.8	± 0.4	3.6	± 0.2	3.1	± 0.4
AT-RetOH	H	Thr48	O	**2.4**	**± 0.1**	**2.4**	**± 0.0**	**2.4**	**± 0.0**
9C-RetOH	H	Thr48	O	**2.5**	**± 0.1**	**2.6**	**± 0.1**	**2.5**	**± 0.1**

[a] *In silico* docking of all-*trans*- (AT) and 9-*cis*- (9C) retinol (RetOH) with human, rat and mouse ADH2. SD is calculated from four different start positions for the docking experiments. Distances important for binding are labeled in bold type. The other distances are not directly related to binding but give a relative position for the substrates close to the active site zinc in the enzymes. C_{15} is the last carbon atom in the retinol chain. H_{15A} and H_{15B} are the hydrogen atoms covalently attached to C_{15}. O and H are the atoms in the hydroxyl group of the substrate (AT-RetOH or 9C-RetOH) or the side chain of Thr48. C_B is the first carbon in the side chain of Thr48. C4N is the *para* position in the nicotinamide ring of the cofactor NAD^+ and it is susceptible to hydride transfer from the substrate.

tor. This differs from other ADHs, which show lower k_{cat} values with retinol isomers than with aliphatic substrates [22].

Since ADH2 is mainly expressed in the liver [27], the kinetic constants strongly suggest that the human enzyme is a major component of the hepatic retinol oxidation. Mouse and rat ADH2 showed much lower activities for retinoids but they could still be of importance for the conversion of retinoids, at least the conversion of 9-*cis*-retinol to 9-*cis*-retinaldehyde in the rat. This conversion has been traced earlier and was described as the remaining non-ADH1 retinol

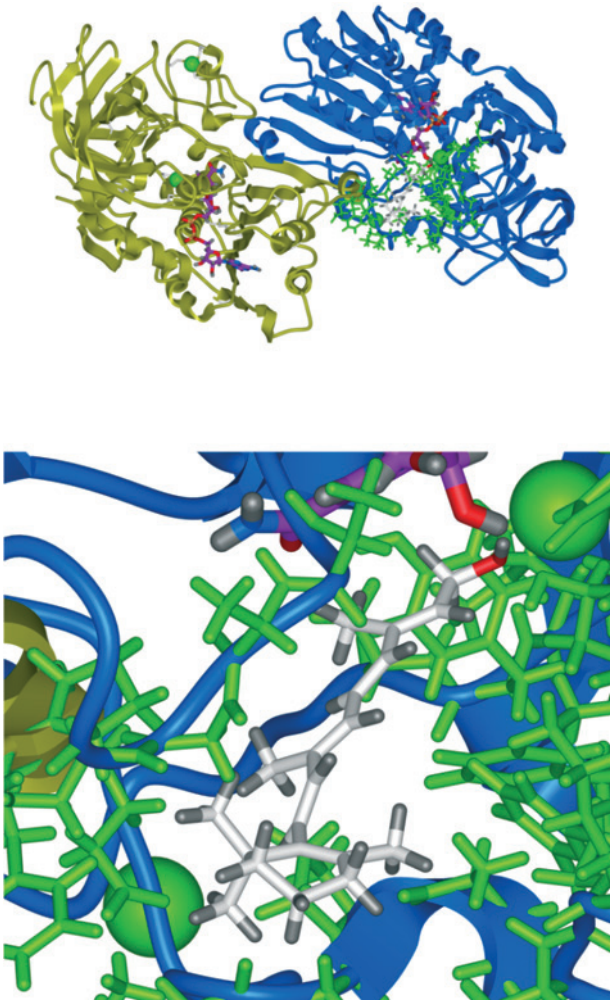

Figure 2. Structural model of human ADH2 with bound all-*trans*-retinol. Human ADH2 is shown as a dimer with one monomer in yellow and one in blue (top). A close-up view of the active site with all-*trans*-retinol is given (bottom). Green residues are the flexible side chains from the docking experiments and zinc atoms are depicted green.

oxidizing capacity of the liver [28]. In line with this, it has been suggested that mouse ADH3 contributes to retinol conversion, although with a very low catalytic ability that is in the same order as that for mouse ADH2 (Table 2). These values should be compared to the corresponding values for ADH1 and ADH4, which are one order of magnitude larger (Table 2, [15]). In contrast to most alcohol/aldehyde pairs, the human and rat ADH2 enzymes showed higher activities for retinols than for retinaldehydes. Similarly, human and mouse ADH4 showed higher turnover for the alcoholic forms of most tested retinoids as compared to the corresponding aldehydes [8, 12, 22]. At the same time human ADH2 has been suggested to participate in the first-pass metabolism of ethanol in the liver, an action that has been shown to competitively inhibit retinol conversion [29].

An additional objective of this study was to explain the large differences in catalytic power in the conversion of retinoids between mouse, rat and human ADH2. The mutation of Pro47 in mouse ADH2 to a His (the residue found in human ADH2) resulted in an increase in retinoid activity towards the values determined for the human enzyme, and this mutation can therefore explain a large part of the difference between species. Similar judgments have been stated for small substrates such as ethanol [16, 18]. However, neither Pro47 in native mouse ADH2 nor His in the mutant ADH2Pro47His (PDB entries 1e3e/1e3l) are close (>3.0 Å) to CXF or the retinoids in the docking experiments. This indicates that the difference in catalytic activity between the mutant and native mouse ADH2 is probably more related to a lowering of the transition state energy barrier for the reactions rather than differences in binding of retinoids. Moreover, the identified isotope effect for mouse ADH2 [16] clearly showed that hydride transfer is rate limiting for alcohol oxidation, *i.e.*, retinol oxidation within this study. This implies that the mutation Pro47His primarily acts by modulation of the hydride transfer step [16]. The docking studies show that all tested retinoids fit well into the substrate pocket of ADH2 in human and rodents, and that no apparent large differences in binding distances between the species could be observed. However, the binding of a substrate is proportional to a change in the free energy, which is difficult to assess from *in silico* methods, thus the results from the docking experiments should be carefully interpreted. The determined K_m values are within a factor of ten between human and rodents compared to a factor of almost 10000 in reaction rates. This further shows that the difference in overall catalytic efficiency between species probably is not related to a large difference in the affinity for retinoids.

The main ADHs that have been proposed to participate in retinoic acid biosynthesis are ADH1 and ADH4 because of their widespread distribution and their high catalytic efficiency [4, 8, 12, 14, 22]. Null mutant mice with metabolic deficiencies for alcohol oxidation provide strong evidence for the role of these ADHs in retinol turnover, albeit with overlapping abilities [30]. Thus, the high levels of ADH1 in liver provide protection against vitamin A toxicity by elimination of the retinol excess. Furthermore, ADH4, distributed in many epithelial tissues, promotes survival during vitamin A deficiency, by generating retinoic acid for essential biological functions [31]. ADH2 activities could not be traced in these experiments due to the very low capacity of the mouse ADH2 to metabolize retinol, a fact that is not valid in

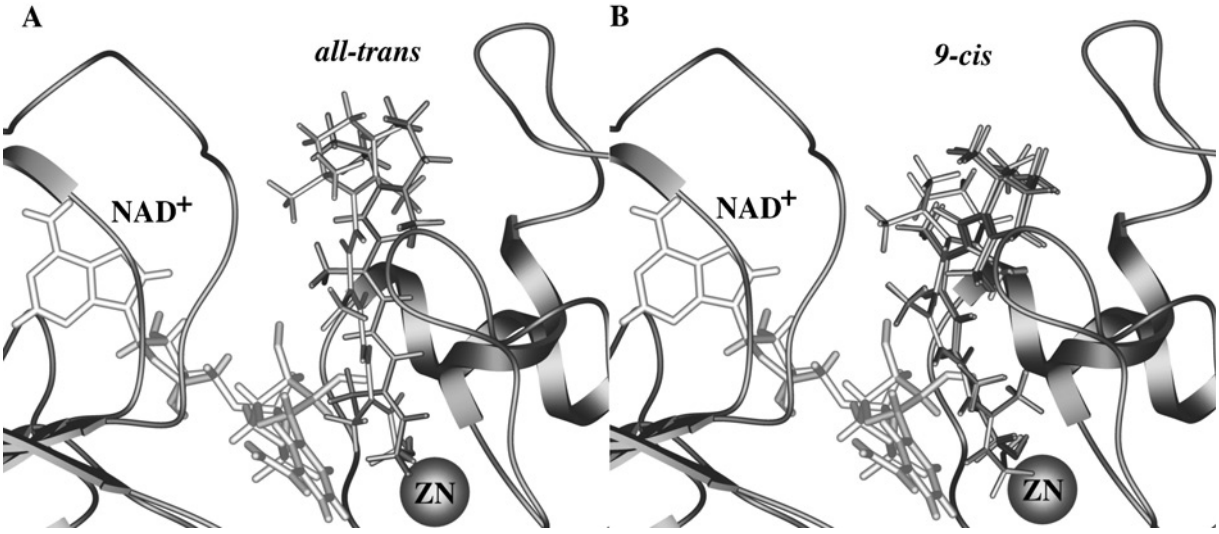

Figure 3. Superposition of all-*trans*- and 9-*cis*-retinol from the docking experiments in human ADH2. The active site showing the final conformation from each of the four dockings of all-*trans* retinol (*A*) and 9-*cis*-retinol (*B*) in human ADH2. The four different conformations from the docking of all-*trans* and 9-*cis*-retinol in human ADH2 display a possible rotation in one plane of about 90 degrees with maintained distance to ZN and NAD^+, see Table 3.

humans where ADH2 is known to be one of the most active forms in the liver [14].

Most retinol in the cell is bound to CRBP and the level of free retinol has been estimated to be less than 0.1 μM [2]. Early experiments have shown that the CRBP-retinol complex is not able to channel to the active site of ADH [32], in contrast to SDR-RDHs, which appeared to use *holo*-CRBP as a substrate [2, 9]. However, a recent overall comparison of enzymes active in all-*trans* retinol/ retinaldehyde conversion (ADH, SDR-RDH and AKR) clearly showed that none of the enzymes studied was active with CRBP-bound retinol/retinaldehyde, but only with free retinol/retinaldehyde [8]. With this comparison under identical conditions, in combination with a sensitive detection method for the formed product, very similar low K_m values were obtained for all-*trans* retinol/ retinaldehyde with enzymes from the different superfamilies. These results set the focus back on ADHs as efficient retinol dehydrogenases, because they show K_m values in the range of physiological levels of free retinol and higher k_{cat} values than the other enzyme groups. This is further supported by studies showing that opposing actions of CRBP and ADH establish a balance between retinol storage and retinol degradation in the liver [10].

In addition, it has been shown that the most common solubilizer for retinoids in several studies, Tween 80, acts as an inhibitor for mammalian ADHs [23]. With the use of BSA instead of Tween 80 as a retinoid solubilizer [8, 19], as in this study, the measured K_m values for retinoids were lowered up to 100-fold for human ADH2, which is in line with the difference obtained for ADH1 and ADH4 in comparison to earlier published data [14, 19, 23, 29].

From the comparison on reaction rates of all-*trans*-retinol/retinaldehyde, human ADH2 can now be added to the list of active human enzymes that at present included ADHs (ADH1 and ADH4), SDR-RDHs and AKRs [8]. Because of its low K_m, ADH2 is one of the most efficient proteins of those compared for the conversion of all-*trans*-retinol at concentrations lower than 0.1 μM in liver. At higher concentrations, the contribution of ADH1 gradually increases because of its higher levels in liver. Thus, ADH2 plays a role in the hepatic elimination of retinol excess, which would be more significant at relatively low retinol concentrations. This is in contrast with its role in ethanol detoxification, where the contribution of ADH2 is more relevant at high ethanol levels, because of its high K_m for this alcohol [33]. This, together with the fact that the catalytic efficiency for conversion of 9-*cis*-retinol is a factor of ten higher than for all-*trans*-retinol, clearly shows that ADH2 is one of the major pathways for conversion of retinols into their corresponding aldehydes in hepatic cells.

Acknowledgements. The Karolinska Institutet is acknowledged for financial support. This work was also supported by grants from the Spanish Dirección General de Investigación (BMC2003-09606, BFU2005-02621) and the Generalitat de Catalunya (2005 SGR 00112).

1 Niederreither, K., Subbarayan, V., Dolle, P. and Chambon, P. (1999) Embryonic retinoic acid synthesis is essential for early mouse post-implantation development. Nat. Genet. 21, 444–448.

2 Napoli, J. L. (1999) Interactions of retinoid binding proteins and enzymes in retinoid metabolism. Biochim. Biophys. Acta 1440, 139–162.
3 Mic, F. A., Molotkov, A., Benbrook, D. M. and Duester, G. (2003) Retinoid activation of retinoic acid receptor but not retinoid X receptor is sufficient to rescue lethal defect in retinoic acid synthesis. Proc. Natl. Acad. Sci. USA 100, 7135–7140.
4 Duester, G. (2000) Families of retinoid dehydrogenases regulating vitamin A function. Production of visual pigment and retinoic acid. Eur. J. Biochem. 267, 4315–4324.
5 Jörnvall, H., Höög, J.-O., Person, B. and Parés, X. (2000) Pharmacogenetics of the alcohol dehydrogenase system. Pharmacology 61, 184–191.
6 Höög, J.-O., Hedberg, J. J., Strömberg, P. and Svensson, S. (2001) Mammalian alcohol dehydrogenase – functional and structural implications. J. Biomed. Sci. 8, 71–76.
7 Crosas, B., Hyndman, D. J., Gallego, O., Martras, S., Parés, X., Flynn, T. G. and Farrés, J. (2003) Human aldose reductase and human small intestine aldose reductase are efficient retinaldehyde reductases: consequences for retinoid metabolism. Biochem. J. 373, 973–979.
8 Gallego, O., Belyaeva, O. V., Porté, S., Ruiz, F. X., Stetsenko, A. V., Shabrova, E. V., Kostereva, N. V., Farrés, J., Parés, X. and Kedishvili, N. Y. (2006) Comparative functional analysis of human medium-chain dehydrogenases, short-chain dehydrogenases/reductases, and aldo-keto reductases with retinoids. Biochem. J. 399, 101–109.
9 Tryggvason, K., Romert, A. and Eriksson, U. (2001) Biosynthesis of 9-*cis*-retinoic acid *in vivo*. J. Biol. Chem. 276, 19253–19258.
10 Molotkov, A., Ghyselinck, N. B., Chambon, P. and Duester, G. (2004) Opposing actions of cellular retinol-binding protein and alcohol dehydrogenase control the balance between retinol storage and degradation. Biochem. J. 383, 295–302.
11 Sirbu, I. O. and Duester, D. (2006) Retinoic-acid signalling in node ectoderm and posterior neural plate directs left-right patterning of somatic mesoderm. Nat. Cell Biol. 8, 271–277.
12 Crosas, B., Allali-Hassani, A., Martinez, S. E., Martras, S., Persson, B., Jörnvall, H., Parés, X. and Farrés, J. (2000) Molecular basis for differential substrate specificity in class IV alcohol dehydrogenases: a conserved function in retinoid metabolism but not in ethanol oxidation. J. Biol. Chem. 275, 25180–25187.
13 Chou, C.-F., La, C.-L., Chang, Y.-C., Duester, G. and Yin, S.-J. (2002) Kinetic mechanism of human class IV alcohol dehydrogenase functioning as a retinol dehydrogenase. J. Biol. Chem. 28, 25209–25216.
14 Yang, Z. N., Davis, G. J., Hurley, T. D., Stone, C. L., Li, T.-K. and Bosron, W. F. (1994) Catalytic efficiency of human alcohol dehydrogenases for retinol oxidation and retinal reduction. Alcohol. Clin. Exp. Res. 18, 587–591.
15 Molotkov, A., Fan, X., Deltour, L., Foglio, M. H., Martras, S., Farrés, J., Parés, X. and Duester, G. (2002) Stimulation of retinoic acid production and growth by ubiquitously expressed alcohol dehydrogenase *Adh3*. Proc. Natl. Acad. Sci. USA 99, 5337–5342.
16 Svensson, S., Strömberg, P. and Höög, J.-O. (1999) A novel subtype of class II alcohol dehydrogenase in rodents. Unique Pro47 and Ser182 modulates hydride transfer. J. Biol. Chem. 274, 29712–29719.
17 Svensson, S., Hedberg, J. J. and Höög, J.-O. (1998) Structural and functional divergence of
class II alcohol dehydrogenase. Cloning and characterization of rabbit liver isoforms of the enzyme. Eur. J. Biochem. 251, 236–243.
18 Svensson, S., Höög, J.-O., Schneider, G. and Sandalova, T. (2000) Crystal structures of mouse class II alcohol dehydrogenase reveal determinants of substrate specificity and efficiency. J. Mol. Biol. 302, 441–453.
19 Belyaeva, O. V., Korkina, O. V., Stetsenko, A. V., Kim, T., Nelson, P. S. and Kedishvili, N. (2005) Biochemical properties of purified human retinol dehydrogenase 12 (RDH12): Catalytic efficiency toward retinoids and C_9 aldehydes and effects of cellular retinol-binding protein type I (CRBPI) and cellular retinaldehyde-binding protein (CRALBP) on the oxidation and reduction of retinoids. Biochemistry 44, 7035–7047.
20 Strömberg, P., Svensson, S., Berst, K. B., Plapp, B. V. and Höög, J.-O. (2004) Enzymatic mechanism of low activity mouse alcohol dehydrogenase 2. Biochemistry 43, 1323–1328.
21 Lapshina E. A., Belyaeva O. V., Chumakova O. V. and Kedishvili, N. Y. (2003) Differential recognition of the free versus bound retinol by human microsomal retinol/sterol dehydrogenases: characterization of the holo-CRBP dehydrogenase activity of RoDH-4. Biochemistry 42, 776–784.
22 Martras, S., Álvarez, R., Martinez, S. E., Torres, D., Gallego, O., Duester, G., Farrés, J., de Lera, A. R. and Parés, X. (2004) The specificity of alcohol dehydrogenase with *cis*-retinoids. Activity with 11-*cis*-retinol and localization in retina. Eur. J. Biochem. 271, 1660–1670.
23 Martras, S., Álvarez, R., Gallego, O., Dominguez, M., de Lera, A. R., Farrés, J., and Parés, X. (2004) Kinetics of human alcohol dehydrogenase with ring-oxidized retinoids: effect of Tween 80. Arch. Biochem. Biophys. 430, 210–217.
24 Moreno, A., Farrés, J., Parés, X., Jörnvall, H. and Persson, B. (1996) Molecular modelling of human gastric alcohol dehydrogenase (class IV) and substrate docking: differences towards the classical liver enzyme (class I). FEBS Lett. 395, 99–102.
25 Vriend, G. (1990) WHAT IF: A molecular modeling and drug design program. J. Mol. Graph. 8, 52–56.
26 Laskowski, R. A., MacArthur, M. W., Moss, D. S. and Thornton, J. M. (1993) PROCHECK: a program to check the stereochemical quality of protein structures. *J. Appl. Cryst.* 26, 283–291.
27 Estonius, M., Svensson, S. and Höög, J.-O. (1996) Alcohol dehydrogenase in human tissues. Localisation of transcripts coding for five classes of the enzyme. FEBS Lett. 397, 338–342.
28 Popescu, G. and Napoli, J. L. (2000) Analysis of rat cytosolic 9-cis-retinol dehydrogenase activity and enzymatic characterization of rat ADHII. Biochim. Biophys. Acta 1476, 43–52.
29 Han, C.-L., Liao, C.-S., Wu, C.-W., Hwong, C.-L., Lee, A.-R. and Yin, S.-J. (1998) Contribution to first-pass metabolism of ethanol and inhibition by ethanol for retinol oxidation in human alcohol dehydrogenase family. Implications for etiology of fetal alcohol syndrome and alcohol-related diseases. Eur. J. Biochem. 254, 25–31.
30 Deltour, L., Foglio, M. H. and Duester, G. (1999) Metabolic deficiencies in alcohol dehydrogenase Adh1, Adh3, and Adh4 null mutant mice. J. Biol. Chem. 274, 16796–16801.
31 Molotkov, A., Deltour, L., Foglio, M. H., Cuenca, A. E and Duester, G. (2002) Distinct retinoid metabolic functions for alcohol dehydrogenase genes Adh1 and Adh4 in protection against vitamin A toxicity or deficiency revealed in double null mutant mice. J. Biol. Chem. 277, 13804–13811.
32 Kedishvili, N. Y., Gough, W. H., Davis, W. I., Parsons, S., Li, T.-K. and Bosron, W. F. (1998) Effect of cellular retinol-binding protein on retinol oxidation by human class IV retinol/alcohol dehydrogenase and inhibition by ethanol. Biochem. Biophys. Res. Commun. 249, 191–196.
33 Bosron, W. F., Li, T.-K., Dafeldecker, W. P. and Vallee, B. L. (1979) Human liver π-alcohol dehydrogenase: kinetic and molecular properties. Biochemistry 18, 1101–1105.